Permeation of nanopores by water: the effects of channel polarization

2003 J. Phys.: Condens. Matter 15 S297

(http://iopscience.iop.org/0953-8984/15/1/340)

INSTITUTE OF PHYSICS PUBLISHING JOURNAL OF PHYSICS: CONDENSED MATTER

J. Phys.: Condens. Matter **15** (2003) S297–S302 PII: S0953-8984(03)54977-3

Permeation of nanopores by water: the effects of channel polarization

Rosalind Allen[1], Simone Melchionna[2] and Jean-Pierre Hansen[1]

[1] Department of Chemistry, University of Cambridge, Lensfield Road, Cambridge CB2 1EW, UK
[2] Istituto per le Applicazioni del Calculo 'M Picone', Consiglio Nazionale delle Ricerche, V le del Policlinico 137, 00161 Rome, Italy

E-mail: rja22@cam.ac.uk (R Allen)

Received 11 October 2002
Published 16 December 2002
Online at stacks.iop.org/JPhysCM/15/S297

Abstract

Molecular dynamics simulations are used to characterize the permeation by water of cylindrical nanopores, modelling ion channels, as a function of channel radius R and dielectric permittivity ϵ. Intermittent permeation is found in a narrow range around the threshold values of R and ϵ. While channel permeation is highly sensitive to channel polarization effects, no effect on structural properties of the confined water is found on varying ϵ.

1. Introduction

Ion channel proteins, embedded in cell membranes, play a crucial physiological role, controlling the transport of ions (essentially K^+, Na^+, Ca^{2+}) and associated water molecules into and out of cells. These proteins have well-conserved amino acid sequences which fold into specific and complicated topologies. However, a general feature is a pore, of typical length $\sim$1 nm and diameter $\leqslant$1 nm, spanning the cell membrane. Such channels therefore provide a unique framework for the study of highly confined fluids and especially ionic solutions. Key questions are those of the permeation of water through the nanopores and the selectivity of competing ionic species.

We consider a highly simplified model of such an ion channel pore, assumed to be a circular cylindrical hole of radius R and length L, through a membrane, which is represented by a slab of dielectric material of permittivity ϵ, separating two reservoirs containing water molecules and ions, as shown in figure 1. Thus the protein and the membrane are treated as a dielectric continuum, which is polarized by the electric charges on the water molecules and ions. In recent publications we have shown that the polarization charge density $\rho_{pol}(\boldsymbol{s})$ which is induced by these charges at position $\boldsymbol{s}$ on the surface of the cylindrical channel can be calculated, for each configuration of water molecules and ions, by minimizing a functional of $\rho_{pol}(\boldsymbol{s})$, which is defined on a surface grid [1, 2]. In a recent letter [3] we combined this variational method for the calculation of the polarization charge with molecular dynamics (MD)

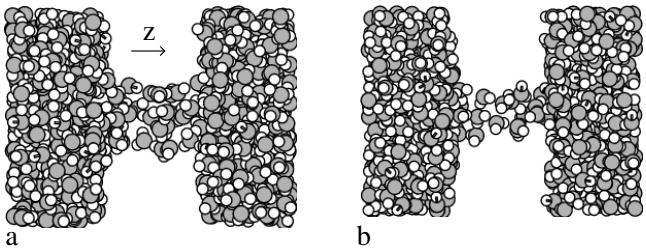

Figure 1. Snapshots from simulations of channels. (a) $R = 0.7$ nm, $\epsilon = 10$. (b) $R = 0.55$ nm, $\epsilon = 10$.

simulations to determine the time-dependent occupancy of the channel by water molecules, the density profiles of water molecules inside the channel and their diffusivity. A striking intermittent permeation of the channel was observed for narrow channels, and the threshold of water permeation was found to be very sensitive to the inclusion of dielectric polarization effects. Further results are presented in this paper, which also examines the disruption of the bulk H-bond network by the confinement. All the results to be presented are for pure water; i.e. no ions are included at this stage.

2. Simulation details

MD simulations were performed on the model described in the introduction and shown in the snapshots of figure 1. The simulation cell is of dimensions $2.6 \times 2.6 \times 3.6$ nm, with periodic boundary conditions being applied in all three directions, connecting the water reservoirs at either end of the simulation cell. The pore length $L = 0.8$ nm and the pore radius R is varied between 0.5 and 0.7 nm. Values for the slab permittivity ϵ between 1 and 10 were tested. Although our earlier simulations [3] were performed with 1068 water molecules [3], we find that half this number is adequate for a bulk-like reservoir and so the results described here are for systems of 534 water molecules. Runs are of typically 1 ns duration. The water in the reservoir regions is maintained at a constant density of 0.996 g cm^{-3} by regular scaling in the z-direction (as indicated in figure 1(a)) of the cell length and of the atomic position vectors, using a version of the Berendsen barostat [4]. A time step of 0.002 ps was used. All the simulations were performed using a modified version of the DL_Protein 2.1 MD code [5].

Interactions between water molecules are described by the SPC/E potential model [6], which consists of a Lennard-Jones (LJ) potential between the O atoms ($\sigma_{\mathrm{O}} = 0.3169$ nm, $\epsilon_{\mathrm{O}} = 0.6502$ kJ mol^{-1}; i.e. $\epsilon_{\mathrm{O}}/k_B = 78.2$ K), and Coulombic interactions between the sites associated with the O atoms ($q_{\mathrm{O}} = -0.8476$) and the two H atoms ($q_{\mathrm{H}} = +0.4238$). All electrostatic interactions between water molecules are calculated using the smooth-particle-mesh Ewald method [7]. The radial interaction between the cylindrical channel surface and the O atoms of the SPC/E water molecules is taken to be the LJ potential between a CH_3 group and an O atom [8], integrated over the volume enclosing an infinitely long cylindrical pore [9]. The same potential, now as a function of the distance d from the planar wall, is used for interactions with the flat surface bounding the reservoirs—shifted in energy to avoid a discontinuity at $d = R$. Appropriate smoothing and rounding is used in the corner regions and at the channel entrance to avoid discontinuities. The 'effective channel radius', R_{eff}, at which the potential energy of a water O atom approaching the wall is equal to k_BT, is $\sim$0.23 nm smaller than the nominal radius R. Likewise the 'effective channel length', L_{eff} is $\sim$0.46 nm longer than L. R_{eff} and L_{eff} are thus quite close to the dimensions of biological ion channels.

Where the dielectric permittivity of the wall is non-trivial, $\epsilon \neq 1$, polarization effects are included using the method alluded to in the introduction, and described in more detail in [1]. A grid is constructed on the cylindrical channel surface with a spacing of 0.05 nm. On the planar surfaces, grids extend 0.45 nm beyond the channel radius and the grid spacing is twice as large as in the channel region. Approximate updates of the polarization surface charge density allow the minimization of the electrostatic functional, which uses the minimum image Green function, to be performed every 100 time steps. These simulations represent an improvement over the results described in a previous paper [3]. In that work, the planar grid spacing was somewhat larger and only water molecules within hemispheres of radius 0.8 nm around the channel mouth contributed to polarization effects. In this work, all molecules are included in the polarization calculation. These modifications lead to a slight shift in the response of the channel to the wall permittivity.

3. Results

The results of the present simulations extend and improve on those presented in [3]. A key result is that channel permeation by water molecules only occurs beyond a threshold radius, for fixed protein permittivity ϵ, and beyond a threshold permittivity, for fixed radius R. Moreover, over a narrow range of R and ϵ around the threshold values, the permeation is intermittent: i.e. periods where the channel is empty alternate with periods where it is filled, on timescales of the order of hundreds of picoseconds or longer. This is illustrated in figure 2, and confirms similar behaviour observed in our earlier work [3], as well as in carbon nanotubes [10] and in more 'realistic' models of ion channels [11]. The threshold is sensitive to the numerical treatment of the protein polarization; as noted in the introduction, compared to our earlier work, we have improved the resolution of the surface grid and included the effects of all water molecules, and this leads to a slight shift of the threshold values of R and ϵ.

A 'map' of empty, intermittent and fully occupied states of the channel in the R–ϵ plane is shown in figure 3. The timescale of the intermittent behaviour is clearly very sensitive to the control parameters in the vicinity of the threshold. If this timescale exceeds the length of our runs (typically 1 ns), the distinction between intermittent and empty or filled states is of course not well defined.

The axial diffusivity of water molecules during periods when a channel is full is surprisingly insensitive to R and ϵ, and similar to bulk diffusion ($D_z \approx 3 \times 10^{-5}$ cm^2 s^{-1}). The rate at which water molecules 'successfully' cross the channel from end to end is quite large, being of the order of 200 ns^{-1}. This rate decreases with R as expected; of course the numbers of crossings are comparable in the two directions, so there is no net flux of water, as expected in an equilibrium simulation.

The radial density profiles of the O atoms of the water molecules are very similar to those reported in [3]: they are rather flat, showing only weak layering near the wall. The present simulations show that these profiles are insensitive to the value of ϵ, i.e. to polarization effects.

Another important issue is how the hydrogen-bonding network that exists between the water molecules is distorted by confinement in the channel. The case of water near a smooth, or molecularly rough, planar wall was examined by Rossky and co-workers [12, 13], but the constraints of confinement are of course much stronger in a cylindrical nanotube. We have examined, among other diagnostics, the variation in the average number of H bonds per molecule with the radial distance r from the cylinder axis. H bonds are defined according to an energetic criterion (interaction between two molecules less than -9.42 kJ mol^{-1} [14]); however, we do not expect the results to be altered qualitatively by the use of an alternative definition. Results for the 0.7 and 0.6 nm channels are shown in figure 4 and compared

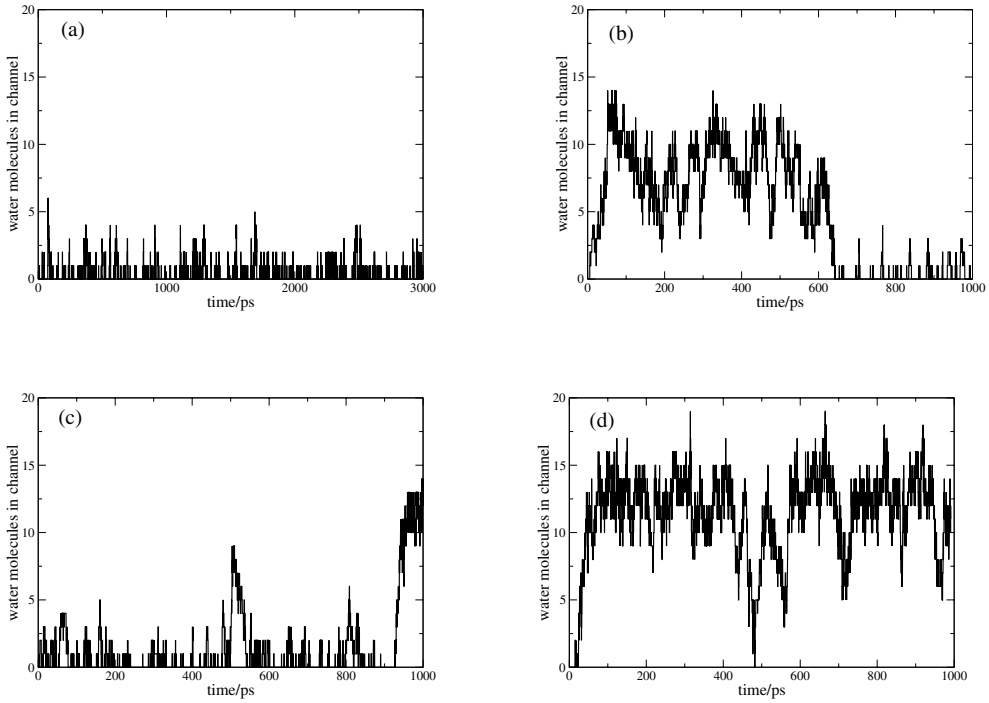

Figure 2. Number of water molecules in the channel as a function of time (in ps). (a) $R = 0.55$ nm, $\epsilon = 1$. (b) $R = 0.55$ nm, $\epsilon = 10$. (c) $R = 0.575$ nm, $\epsilon = 4$. (d) $R = 0.6$ nm, $\epsilon = 4$. Note the change in scale on the time axis in (a). Simulation (a) was performed with 1068 water molecules; the others were with 534 molecules.

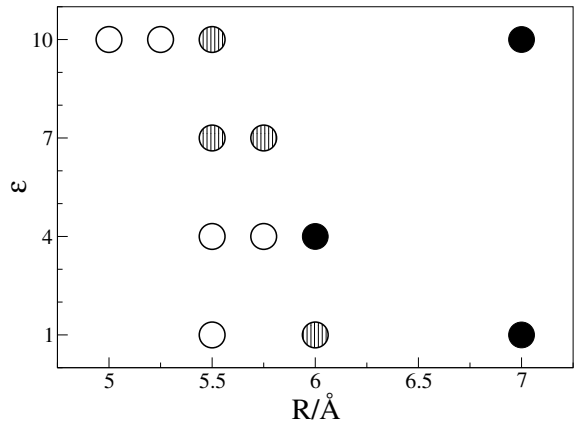

Figure 3. A diagram showing the results of a series of simulation runs at various values of ϵ and R for a channel of length $L = 0.8$ nm ($L_{eff} = 1.26$ nm). Open circles indicate that no filling events were observed; stripes indicate intermittent filling and filled circles show channels that remained full for the duration of the run. Runs were $\sim$1 ns or longer in length.

to the corresponding profiles obtained for a cylinder of radius R_{eff} cut from a bulk water sample run under the same conditions. To obtain the 'bulk' profiles, all molecules whose O atoms are outside the cylindrical boundary are ignored—thus no H bonds which cross the

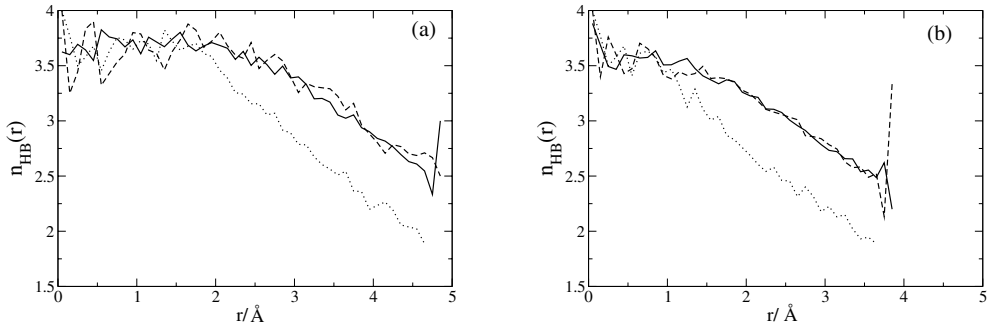

Figure 4. Average number of H bonds per molecule $n_{\mathrm{HB}}(r)$ as a function of radial distance r. (a) $R = 0.7$ nm ($R_{eff} = 0.47$ nm), $\epsilon = 1$ (——) and $\epsilon = 10$ (- - - -). (b) $R = 0.6$ nm ($R_{eff} = 0.37$ nm), $\epsilon = 1$ (——) and $\epsilon = 4$ (- - - -). Averaging is over times when channels are full. The dotted curves (· · · · · ·) show the results obtained for a cylinder of radius R_{eff} cut from a bulk water sample run under the same conditions.

boundary are included. The mean number of H bonds formed by the confined water decreases as the surface of the cylinder is approached, as one might expect since fewer neighbouring molecules are available for bonding. However, this number is always above the 'bulk' value, showing that the water molecules deviate from their bulk configuration so as to strengthen their H-bonding network close to the surface. This tendency was also observed by Rossky and co-workers [12, 13] for the planar geometry. It is also to be noted that protein polarization has practically no effect on the profiles.

4. Conclusions

We have characterized the permeation of cylindrical nanopores of finite length (a model for ion channels) by water molecules, using MD simulations. Earlier conclusions have been sharpened by improving the grid in the variational calculation of the polarization charge induced on the channel surface, and by extending the range of the control parameters R and ϵ. Whilst structural properties of the confined water are little affected by the surface polarization, the collective behaviour depends strongly on ϵ, which was varied in the MD simulations between $\epsilon = 1$ (non-polarizable protein) and $\epsilon = 10$ (a reasonable value for many channel proteins). In particular, the permeability threshold for a given radius R is very sensitive to ϵ, permeation being facilitated by the dielectric effects.

Future work will include cations (which are expected to favour water permeation [3]), and explore non-equilibrium situations, with concentration gradients across the membrane, which are very important in biological systems.

Acknowledgments

The authors acknowledge useful discussions with Professor R Eisenberg. RA is grateful to the EPSRC for funding and to Unilever for a CASE award.

References

[1] Allen R, Hansen J-P and Melchionna S 2001 *Phys. Chem. Chem. Phys.* **3** 4177
[2] Allen R and Hansen J-P 2002 *J. Phys.: Condens. Matter* at press

[3] Allen R, Melchionna S and Hansen J-P 2002 *Phys. Rev. Lett.* **89** 1755502
[4] Berendsen H J C, Postma J P M, van Gunsteren W F, DiNola A and Haak J R 1984 *J. Chem. Phys.* **81** 3684
[5] Melchionna S and Cozzini S 2001 *DL_Protein 2.1 User Guide*
[6] Berendsen H J C, Grigera J R and Straatsma T P 1987 *J. Phys. Chem.* **91** 6269
[7] Essmann U, Perera L, Berkowitz M L, Darden T, Lee H and Pedersen L G 1995 *J. Chem. Phys.* **103** 8577
[8] Martin M G and Siepmann J I 1998 *J. Phys. Chem.* B **102** 2569
[9] Peterson B K, Walton J P R B and Gubbins K E 1986 *J. Chem. Soc. Faraday Trans. II* **82** 1789
[10] Hummer G, Rasaiah J C and Nowortya J P 2001 *Nature* **414** 188
[11] Beckstein O, Biggin P C and Sansom M S P 2001 *J. Phys. Chem.* B **105** 12902
[12] Lee C Y, McCammon J A and Rossky P J 1984 *J. Chem. Phys.* **80** 4448
[13] Lee S H and Rossky P J 1994 *J. Chem. Phys.* **100** 3334
[14] Jorgensen W L, Chandrasekhar J, Madura J D, Impey R W and Klein M L 1983 *J. Chem. Phys.* **79** 926